Supporting Information for “Photonic Welding Points for Arbitrary On-Chip Optical Interconnects”

Zejie Yu, Yang Ma, and Xiankai Sun*

Department of Electronic Engineering, The Chinese University of Hong Kong, Shatin, New Territories, Hong Kong
**Corresponding author: xksun@cuhk.edu.hk*

A. Loss Analysis of Waveguide Bends

Figure S1A illustrates a waveguide bend connecting two straight waveguides, where s and r denote the directions of along and perpendicular to the waveguide, respectively. The loss introduced by a waveguide bend that connects two straight waveguides consists of two main contributions: modal mismatch at the joints and bending loss along the bend. The electric field distributions of the fundamental TE mode in a straight and bent waveguide are shown in Figures S1B and S1C. It is clear that the mode in the straight waveguide is symmetric with respect to its central line while the mode in the bent waveguide shifts to the outer corner. The modal overlap factor can be expressed as

$$\xi = \frac{\left|\iint \mathbf{E}_s^* \mathbf{E}_b drdz\right|}{\sqrt{\left|\iint \mathbf{E}_s^* \mathbf{E}_s drdz\right|\left|\iint \mathbf{E}_b^* \mathbf{E}_b drdz\right|}}, \tag{S1}$$

where $\mathbf{E}_s$ and $\mathbf{E}_b$ represent the cross-sectional modal electric field in the straight and bent waveguides, respectively. We simulated the modal profiles for straight and bent silicon waveguides sitting on oxide, where the waveguide width and height are 500 nm and 220 nm, respectively. Figure S2 shows the modal overlap factor ξ as a function of the bend radius. It is clear that ξ decreases dramatically when the bend radius becomes very small, which contributes significantly to the insertion loss as light travels from a straight waveguide to a bent waveguide.

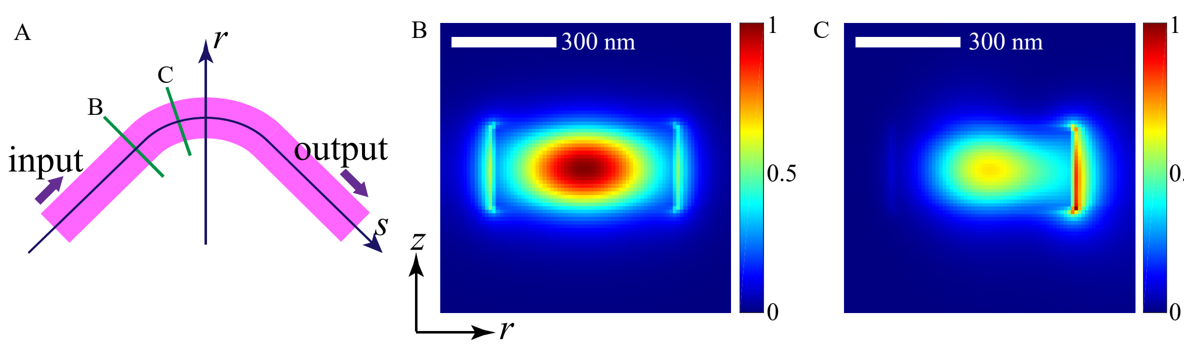

Figure S1: (A) Illustration of a waveguide bend connecting two straight waveguides. (B) Electric field distribution ($|\mathbf{E}_s|$) of the fundamental TE mode in the straight waveguide. (C) Electric field distribution ($|\mathbf{E}_b|$) of the fundamental TE mode in the waveguide bend.

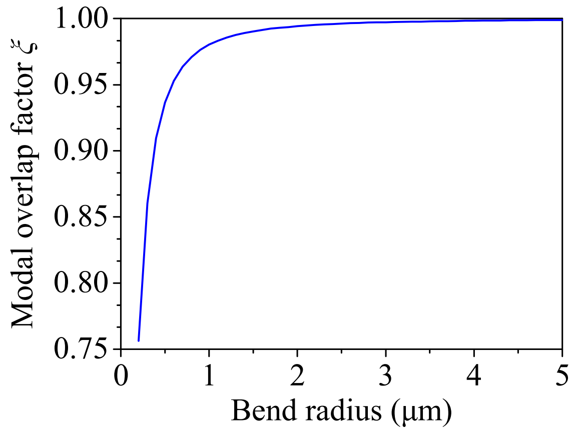

Figure S2: Overlap factor ξ of the modal electric fields in a straight and a bent waveguide as a function of the inner radius of the bent waveguide.

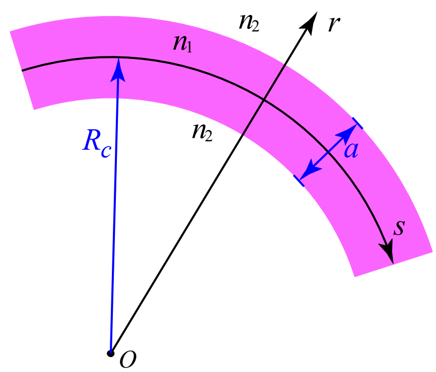

Figure S3: Illustration of a waveguide bend. R_c and a are the radius and width of the waveguide bend, respectively. n_1 and n_2 are the refractive indices of the waveguide bend and the surrounding medium, respectively.

For waveguide bends with a step-index profile as shown in Figure S3, the electric fields E_r and E_z can be expressed as [1]

$$\begin{cases} E_r(r) = h_s^{-3/2} F(r) \exp(i\beta s) & \text{for TE mode,} \\ E_z(r) = h_s^{-1/2} F(r) \exp(i\beta s) & \text{for TM mode,} \end{cases} \tag{S2}$$

where $h_s = 1 + r/R_c$ and $F(r)$ satisfies

$$\frac{d^2F}{dr^2} + \left[k_0^2 n^2(r) - \beta_e^2 / h_s^2\right] F = 0 \tag{S3}$$

with $\beta_e^2 = \beta^2 - 1/(2R_c)^2$.

The behavior of Eq. (S3) can be explained by the tunneling leaky modes as shown in Figure S1C. We can employ the ordinary WKB tunneling theory to evaluate the imaginary part of the propagation constant β in Eq. (S2) as the waveguide under consideration has a step-index distribution [2]. The obtained radiation loss for light in a bent waveguide can be expressed as

$$\alpha = T_f \frac{\exp\left[-4\int_{a/2}^{r_c} w_e(r)/(h_s a)dr\right]}{\beta a\int_0^{a/2}\left[u_e(r)h_s\right]^{-1} dr}, \tag{S4}$$

where $u_e(r) = a(k_0^2 n_1^2 h_s^2 - \beta_e^2)^{1/2}/2$, $w_e(r) = a(\beta_e^2 - k_0^2 n_2^2 h_s^2)^{1/2}/2$, $x_c = R_c[\beta_e/(k_0 n_2) - 1]$, and T_f is the Fresnel transmission coefficient at the interface due to index discontinuity in slab waveguides:

$$T_f = \begin{cases} \dfrac{4u_e(a/2)w_e(a/2)n_1^2 n_2^2}{n_2^4 u_e^2(a/2) + n_1^4 w_e^2(a/2)} & \text{for TE mode,} \\ \dfrac{4u_e(a/2)w_e(a/2)}{u_e^2(a/2) + w_e^2(a/2)} & \text{for TM mode.} \end{cases} \tag{S5}$$

The integrals in Eq. (S4) can be solved analytically, yielding

$$\alpha = K\exp(-SR_c) \tag{S6}$$

with

$$K = \frac{u_e(a/2)}{\beta a^2/2} T_f \tag{S7}$$

and

$$S = 2\beta\left\{\tanh^{-1}\left[\frac{w_e(a/2)}{\beta_e a/2}\right] - \frac{w_e(a/2)}{\beta_e a/2}\right\}. \tag{S8}$$

Therefore, Eq. (S6) clearly shows that the bending loss increases as the radius of a waveguide bend reduces.

B. Supplementary Data for Design and Simulation of Photonic Welding Points

The method described in the main manuscript can be used to design photonic welding points for connecting waveguides intersecting at an arbitrary angle with a very low loss in a wide band. Besides the experimental results in the main manuscript, here we provide the design and simulated performance of photonic welding points for connecting two straight waveguides with the bending angle of 15°, 45°, 75°, 105°, 135°, and 165°. The profiles of the designed structures and the corresponding normalized transmission spectra are plotted in Figures S4A and S4B, respectively.

Figure S5 presents zoomed-in views of the photonic welding points inside the green regions in Fig. 2A, which are used for connecting two waveguides with the bending angle of 30°, 60°, 90°, 120°, and 150°.

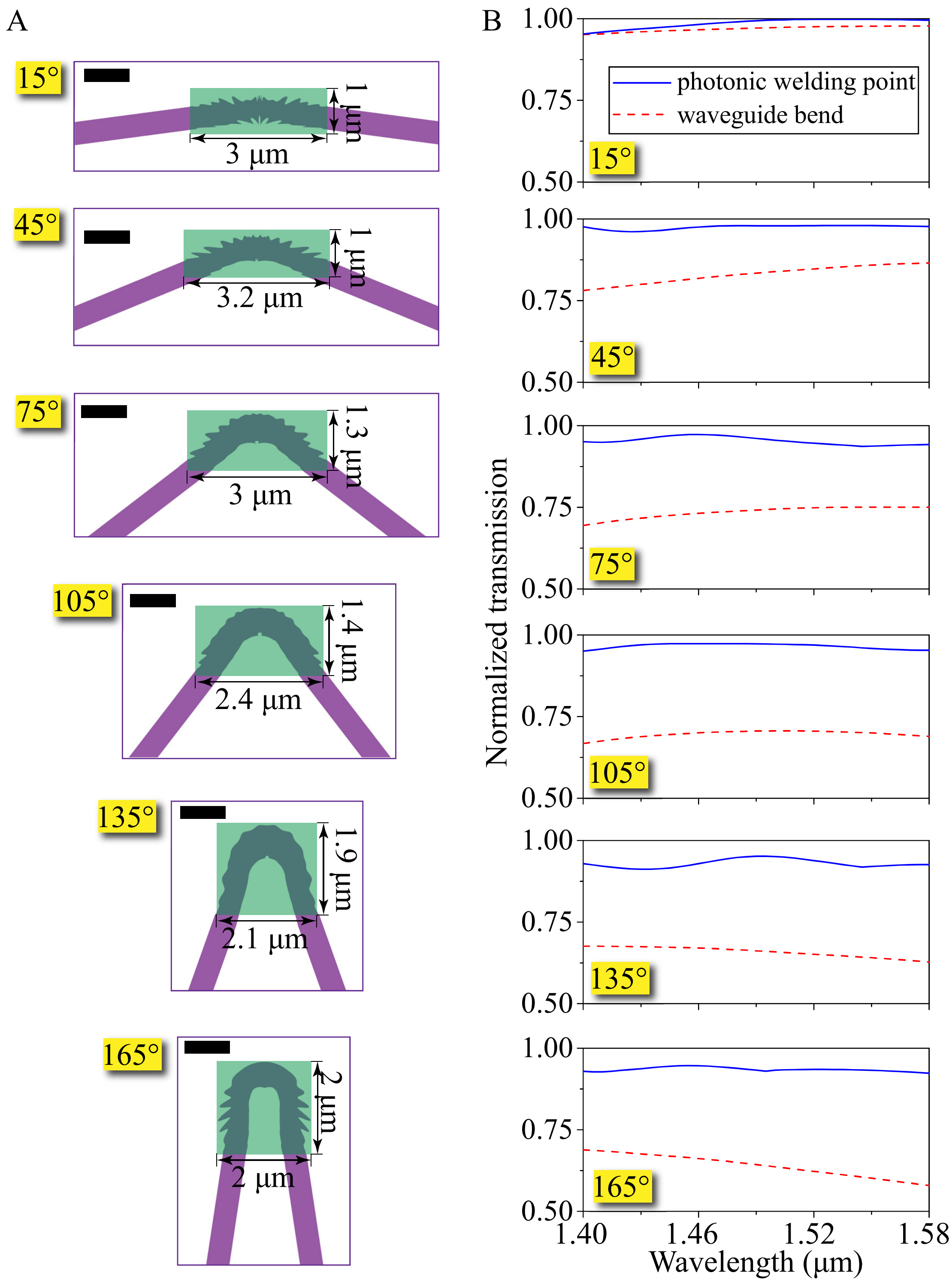

Figure S4: (A) Designed structures of photonic welding points for connecting two waveguides with the bending angle of 15°, 45°, 75°, 105°, 135°, and 165°. All the scale bars represent 1 μm. (B) Normalized transmission spectra of the photonic welding points (blue solid lines) and waveguide bends (red dashed line) for connecting two waveguides with the bending angle of 15°, 45°, 75°, 105°, 135°, and 165°.

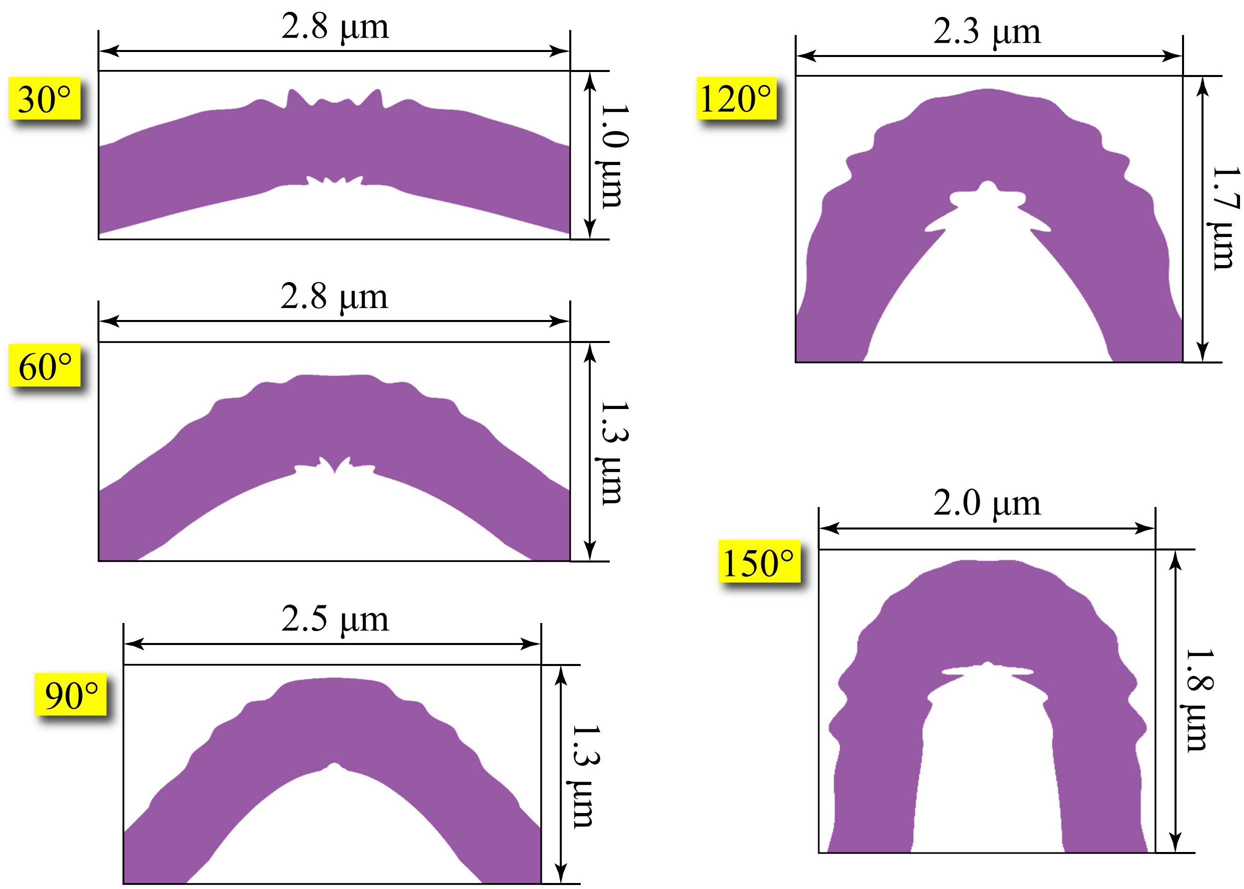

Figure S5: Zoomed-in views of the photonic welding points inside the green regions in Fig. 2A, which are used for connecting two waveguides with the bending angle of 30°, 60°, 90°, 120°, and 150°.

References

[1] Cheng YH, Lin WG. Radiation loss in bent step-index slab waveguides. Opt Lett 1989, 14, 1231–1233.

[2] Love JD, Winkler C. Attenuation and tunneling coefficients for leaky rays in multilayered optical waveguides. J Opt Soc Am 1977, 67, 1627–1633.